INTERNATIONAL SOCIETY FOR
SOIL MECHANICS AND
GEOTECHNICAL ENGINEERING

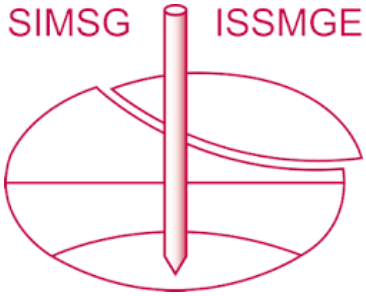

This paper was downloaded from the Online Library of the International Society for Soil Mechanics and Geotechnical Engineering (ISSMGE). The library is available here:

https://www.issmge.org/publications/online-library

This is an open-access database that archives thousands of papers published under the Auspices of the ISSMGE and maintained by the Innovation and Development Committee of ISSMGE.

Large deformation analysis of rectangular plate anchors in normally consolidated clay

Dong Wang, Yuxia Hu, Zhenhe Song
Department of Civil Engineering, Curtin University of Technology, Perth, WA, Australia

Keywords: plate anchor, finite elements, large deformation, capacity, clay

ABSTRACT

The performance of rectangular plate anchors in normally consolidated clay has been studied using three-dimensional large deformation finite element analysis. The large deformation FE method has been extended from 2D to 3D case to study the effect of anchor shape. The large deformation analysis is based on mesh regeneration and interpolation of stresses and material parameters, in which a modified "Recovery by Equilibrium in Patches technique" is developed to improve the accuracy of stress mapping. Anchors with a range of aspect ratios were modelled under no-breakaway and immediate breakaway conditions, using small strain and large deformation FE methods. It was found that the anchor aspect ratio has a significant effect on anchor capacity. However, the soil strength gradient, k, has no effect on anchor capacity in the range of k = 1 to 3 kPa/m. The depth at which separation between soil and anchor occurs was found to be deeper for normally consolidated soil with strength proportional to depth than for uniform strength soil

1 INTRODUCTION

Plate anchors are potential anchorages to moor large floating structures in offshore engineering, especially in deep water developments. Suction caisson installation of plate anchors has become a popular option (Wilde et al. 2001). Restricted by the length-to-diameter ratio of caissons, most suction embedded plate anchors in practice are rectangular in shape rather than circular or strip, although the latter shapes have been most analysed due to their simpler two-dimensional geometry. A variety of laboratory tests and theoretical analyses have been performed to study the pullout capacity of plate anchors. In a series of small scale model tests (Das 1980; Das and Singh 1994) an immediate breakaway condition was ensured by venting the back face of the anchor by means of a hollow pipe placed vertically beneath the anchor. From the results of these tests, they proposed that the pullout capacity may be expressed as the sum of overburden pressure above the anchor and the corresponding capacity in weightless soil. However, the anchor capacity cannot increase indefinitely with the overburden pressure, since a limiting resistance is ultimately reached due to a local flow mechanism around the anchor. A limiting bearing capacity, independent of overburden stress, must therefore be placed on the approach suggested by Das. Merifield et al. (2001, 2003) used finite element (FE) formulations of the limit theorems to evaluate the effect of overburden pressure, anchor shape and roughness. Exact solutions are available for deep thin circular anchors, for the no-breakaway case, where soil is attached to the anchor base (Martin and Randolph 2001).

Previous analytical studies have mainly focused on anchors in uniform strength clay. However, practical applications in deep water are generally in normally consolidated (NC) or lightly over-consolidated clay where the undrained strength s_u typically increases linearly with depth

$$s_u = s_{um} + kz \quad (1)$$

where s_{um} is the soil strength at the mudline; k is the strength gradient; and z is the soil depth. Typically, k is less than 3 kPa/m. From two-dimensional anchor studies with continuous pullout with breakaway allowed, it has been found that, both in uniform and NC clays, the ultimate capacity may require significant anchor displacement before it is mobilised (Song and Hu 2005). In such cases conventional small strain FE analysis and plastic limit analysis cannot predict accurately the capacity development during continuous pullout.

In this paper, the behaviour of rectangular anchors in NC clay is studied using a three-dimensional large deformation FE approach that incorporates mesh regeneration to avoid severe element distortion. The numerical results are compared with centrifuge test data and analytical solutions.

The variation of capacity factors with embedment ratio is investigated for no breakaway and immediate breakaway cases. The separation between the anchor base and the soil underneath can be tracked in the large deformation simulation, allowing the separation depth to be quantified.

2 LARGE DEFORMATION FINITE ELEMENT PROCEDURE

Although small strain FE analysis has been used widely in the determination of anchor capacities (Rowe and Davis 1982), the accuracy of this approach, which is based on a Lagrangian formulation, is suspect where large displacements are required to mobilise the ultimate capacity. This is due to distortion of the FE mesh in the vicinity of the anchor. More importantly, however, the small strain approach cannot take account of geometric changes as the anchor moves upwards toward the free surface, and potentially into soil of lower strength. Hu and Randolph (2002) have presented a two-dimensional large deformation approach, Remeshing and Interpolation Technique with Small Strain (RITSS), to obtain the bearing capacity of skirted foundations. Circular and strip plate anchors were also treated with this approach (Song and Hu 2005). Here RITSS is extended to three-dimensional problems, and the basic procedure is as follows: (1) The continuous pullout process is divided into a series of incremental analyses. At the beginning of each increment, the deformed soil domain is re-meshed. ABAQUS is adopted due to the three-dimensional nature of the analysis. Two Python files are coded to track the deformed geometry of the soil domain and to control the automatic mesh generation, Python being the built-in script language of ABAQUS. (2) After mesh regeneration, the stress components and soil parameters are mapped from the old mesh to the new mesh. When extended to three-dimensional analysis, the superconvergent patch recovery method and modified unique element method adopted in the two-dimensional RITSS method for stress mapping becomes complex due to the lack of confidence in superconvergent points in tetrahedron elements. Instead, an alternative technique called "Recovery by Equilibrium in Patches (REP)" was modified and introduced into the three-dimensional calculations. A full description of REP can be found in Borromand and Zienkiewicz (1997) and only our modification is described briefly here. Our aim is to improve the accuracy of recovered stresses on the boundary nodes. Considering the difficulty in meshing deformed domains with irregular boundaries, quadratic tetrahedrons rather than brick elements were chosen. Since boundary nodes cannot be used as the patch assembly node in REP, elements with all nodes on boundaries was not involved in any element patch. For this kind of special element, stress components on vertex nodes are extrapolated from the Gauss points in the same element. The stresses on each mid-side node are derived by averaging the corresponding values on the 2 adjacent vertex nodes. Stresses on the new Gauss point are then deduced from nodes of the surrounding old element. The marine clay under undrained condition may be modelled as an elasto-perfectly plastic material with Tresca yield criterion. Young's modulus E is taken as $500s_u$. Poisson's ratio is 0.49 to approximate constant soil volume. The buoyant unit weight of soil is represented as γ' and the coefficient of lateral earth pressure has been taken here is 1. The constitutive parameters s_u and E also need to be recovered during mesh regeneration, as the strength varies with depth. (3) The mapped stresses and soil parameters are input into ABAQUS through user subroutine interfaces. The plate anchor is pulled up for a prescribed distance in each increment, with the distance small enough to avoid excessive mesh distortion. A small strain calculation is carried out in ABAQUS to get the response of the anchor over this incremental displacement. (4) The above steps are repeated until the anchor is pulled to a predefined embedment. To make this procedure running automatically and continuously, a Fortran program was developed to call ABAQUS and the Fortran subroutines implementing recovery of the stress and soil parameters.

In the following large deformation calculations, rectangular anchors with aspect ratios, L/B, of 1 and 2 are considered, where L and B are the anchor length and width, respectively. The anchor thickness is taken as t = B/40. The current and initial embedment of the anchor are written as H and H_i. The interface between anchor and soil is assumed to be completely rough, although breakaway is allowed on the back face of the anchor (after which the exposed soil surface becomes free of traction). The strength at the mudline is taken as $s_{um} = 0$. The plate capacity factor $N_{c\gamma}$ is obtained by normalising the maximum anchor resistance, F_{max}, by the anchor area, A, and the soil strength, s_{u0}, at the initial anchor embedment, to give

$$N_{c\gamma} = F_{max}/As_{uo} \tag{2}$$

For weightless soil, the capacity factor is expressed as N_{co}.

3 COMPARISON WITH CENTRIFUGE TEST

Recently, the rotation behaviour of square inclined anchors was investigated in centrifuge tests conducted at the Centre for Offshore Foundation Systems, University of Western Australia. The kaolin clay sample was normally consolidated for 90 hours in the beam centrifuge under an acceleration of 100g. The results of six T-bar tests prior to the pullout are illustrated in Figure 1, and give an average s_{um} of zero and strength gradient of $k = 1.5$ kPa/m. The T-bar factor was adopted as 10.5. The close grouping of the T-bar tests, which were conducted over a period of several days during the anchor tests, shows the sample was well consolidated from the start of the pullout tests. The prototype anchor was 4 m wide and 0.2 m thick. It was initially inserted vertically (with the centrifuge at rest) to the desired depth using an installation device. After res-starting the centrifuge and allowing a period of reconsolidation, the anchor chain connected the anchor shank was pulled out vertically at a rate of $v = 0.5$ mm/s thus giving a dimensionless velocity, vB/c_v (where c_v is the consolidation coefficient), in excess of 30 to ensure undrained behaviour. The anchor rotated gradually to the horizontal before moving upwards. It was observed that the capacity development of the anchor comprised four phases (Figure 2): phase 1, chain tightening; phase 2, anchor rotation; phase 3, pullout capacity development with anchor fully rotated; and phase 4, anchor pullout with full capacity. This is in accordance with the observations reported for anchors in uniform soil (Song et al. 2006). The maximum capacity occurs at the end of phase 3. The reduction of anchor capacity towards the soil surface in phase 4 is due to the decreasing soil strength. In the large deformation analyses reported here, only the pull-up process was simulated and the anchor was placed horizontally at the initial embedment.

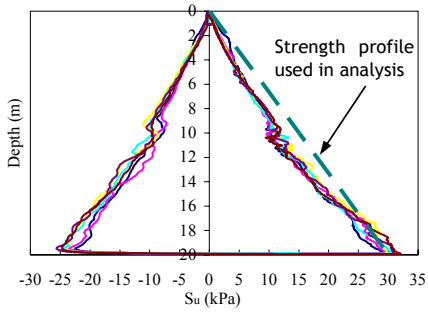

Figure 1: Results of six T-bar tests

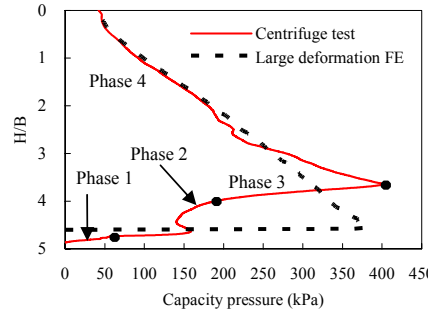

Figure 2: Comparison between model test and FE

Inspection of the hole in the soil sample induced by the anchor pullout indicated the soil remained attached to the anchor base even when the anchor was pulled up near the soil surface, which means the suction force was fully sustained. In accordance with the test phenomenon, the large deformation FE was conducted under no breakaway condition. Due to initial rotation of the model anchor in the centrifuge test, an approximate initial embedment had to be chosen for the FE comparison. An initial embedment ratio of $H_i/B = 4.6$ was chosen for the large deformation analysis. The mobilized capacities from centrifuge test and large deformation analysis are compared in Figure 2. Although the anchor rotation was not simulated, the large deformation analysis offers consistent capacity development with the test data. The maximum anchor capacity pressure from the FE analysis is 381 kPa, only 5 % lower than the centrifuge result.

4 NO BREAKAWAY CASES

To benchmark the three-dimensional large deformation program, a circular plate anchor in NC clay was analysed, even though a two-dimensional analysis would have been sufficient due to axial symmetry. The exact capacity factor for a deeply embedded ultra thin circular plate is $N_{co} = N_{c\gamma} = 13.11$ (Martin and Randolph 2001). The load-displacement curves of a circular anchor with thickness $t/D = 40$ and initial embedment $H_i/D = 3$, are shown in Figure 3, where D is the anchor diameter and γ' is taken as 7 kN/m^3. In both uniform and NC clays, the anchor capacity factor reaches the maximum value immediately after the anchor pullout. The capacity factor is 14.05 (7.2% greater than the exact solution) for uniform clay and 13.91 for NC clay. The results verify the reliability of the large deformation analysis.

Meanwhile, the load-displacement curve from conventional small strain FE analysis based on the same initial mesh as for the large deformation analysis, is also included in Figure 3. Small strain FE cannot derive ultimate capacity due to the computing non-convergence. Furthermore, the mobilised capacity factor keeps increasing, which contrasts with the phenomenon observed in the centrifuge tests (Figure 2). The advantage of large deformation analyses over small strain FE is obvious in predicting the capacity of anchors in NC clay.

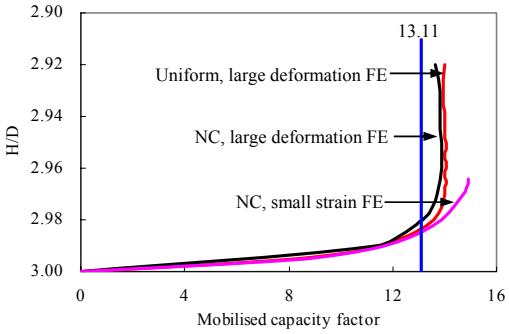

Figure 3: Normalised capacity factor of circular anchors in uniform clay and NC clay

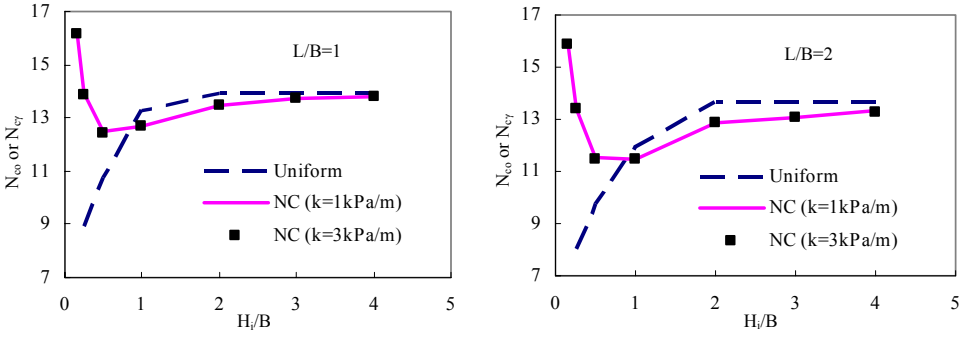

Figure 4: Capacity factors of rectangular anchors under no breakaway condition

For rectangular anchors, the variation of capacity factor at different initial embedment is displayed in Figure 4. Under no breakaway condition, the overburden pressure imposed on the anchor top is balanced by that on the anchor base, so the unit weight of soil has no effect on pullout capacities, $N_{co} = N_{c\gamma}$. The capacity factor in uniform clay always decreases with decreasing embedment ratio, while the factor tends to increase when the anchor in NC clay is near the mudline. This is due to the lower soil strength, s_{uo} corresponding to the initial embedment, used in calculating the capacity factor in Eq. 2. The strength gradient of NC clay has no effect on the capacity factors in the range of k = 1 to 3 kPa/m ($k/\gamma' = 0.14$ to 0.43). At a specified embedment ratio, the factor decreases with the increase of aspect ratio for both uniform clay and NC clay by (2~12)%.

5 IMMEDIATE BREAKAWAY CASES IN WEIGHTLESS SOIL

Where breakaway is allowed, the anchor base separates immediately from the soil once the pulling load is applied if the overburden pressure is insignificant. The capacity of anchors in practice will be always greater than that calculated for weightless soil. For weightless soil, as shown in Figure 5, the capacity factor in NC clay is less than that in uniform clay, especially for shallow anchors. Under immediate breakaway condition, the soil extending to the free surface above the anchor is mobilised to resist the pulling force. For NC clay, the ratio of the average strength above the anchor to the local strength at the anchor increases as the anchor embedment is deeper. So the capacity factor of deep anchors in NC clay tends to be close to that in uniform clay, and the latter is the upper limit of the former. As well as no breakaway cases, the influence of strength gradient on the capacity factor N_{co} of vented cases can be neglected. The capacity factor of anchors in NC clay is reduced (12~25)% when its aspect ratio increase from 1 to 2. By comparing the N_{co} values in Figures 4 and 5, it is observed that anchor capacity may be improved significantly when a suction force can

be sustained. Thus, it is important to try to identify a separation depth, and $N_{c\gamma}$ for no-breakaway case can be used before separation.

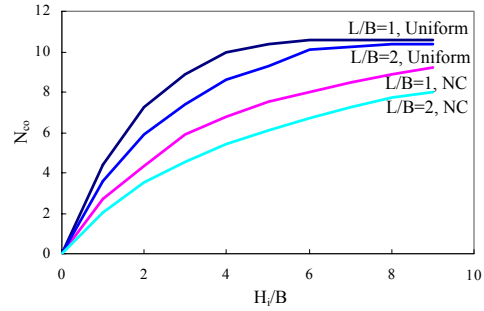

Figure 5: Breakout factors of rectangular anchors in weightless soil

6 SEPARATION DEPTH

When soil weight is considered, soil will tend to attach to the anchor at deep embedment due to the high overburden pressure around anchor. However, soil may separate from the anchor at shallow embedment due to the reduced overburden pressure. Thus, the large deformation analysis can simulate the continuous pullout process by assessing the "anchor base-soil" contact condition. The contact conditions consist of full attachment at the beginning of loading at deep embedment and gradual separation when embedment is decreased during pullout. Note that in these analyses, separation is allowed once the normal stress drops to zero, although in the actual soil, transient suctions (or reduction in hydrostatic pore pressure) may be sustained, particularly in deep water.

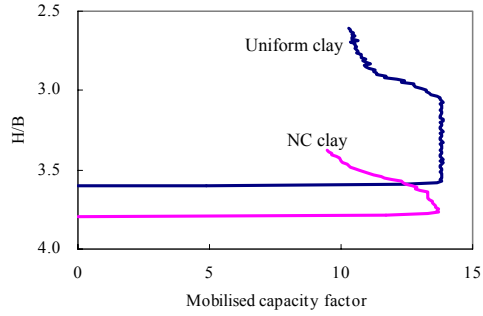

Figure 6: Continuous pullout process in uniform clay and NC clay

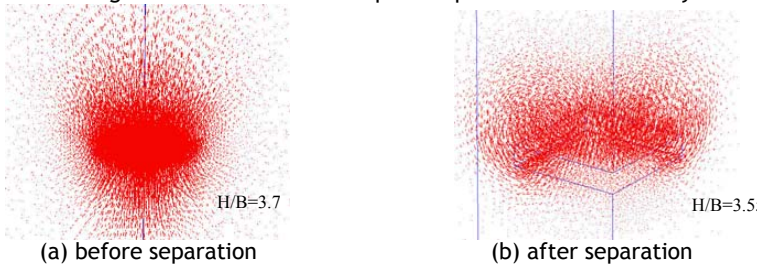

(a) before separation (b) after separation

Figure 7: Soil flow mechanisms before and after the separation in NC soil

For the idealised conditions, with separation assumed to occur once the normal stress on the back face of the anchor reduces to zero, the separation depth H_s may be related to anchor geometry, soil (effective) unit weight and soil strength gradient. For a square anchor of width 6 m, embedded in uniform strength clay with s_u = 21 kPa, at an initial embedment ratio of H_i/B = 3.6, separation occurs at H_s=3.05B as shown in Figure 6. If the same anchor is placed in NC clay with k = 0.921 kPa/m (in both cases with γ' = 7 kN/m^3) and initial embedment H_i = 3.8B, the soil strength at the embedment is also 21 kPa. The separation depth in NC clay is H_s = 3.63B, which is deeper

than that in uniform clay. The reason is that in NC clay, the soil strength and elastic modulus is lower above the anchor, so that a surface failure mechanism is reached sooner. For NC clay, the soil flow mechanisms at H/B = 3.7 and 3.55 are plotted in Figure 7. A local domain with great displacement is formed around the anchor before the separation, and the displacement of soil beneath the anchor base is negligible after the separation. The FE results in Figures 6 and 7 have displayed a clear separation depth. However, the transient suctions in centrifuge tests are easily sustained during pullout, so there is no separation in Figure 2.

7 CONCLUSIONS

The pullout capacity of rectangular anchors has been investigated using a three-dimensional large deformation FE method. The reliability and accuracy of the approach was verified by comparison with centrifuge test data and limit analysis solutions. Under no breakaway condition, the anchor capacity factor is reduced (2~12)% when its aspect ratio increase from 1 to 2; under immediate breakaway condition, the reduction is (12~25)% for NC clay. Under no breakaway condition, soil strength gradient showed no effect on anchor capacity in the range of $k/\gamma' = 0.14$ to 0.43. In large deformation analysis, when soil strength at the embedment depth is kept the same, the separation depth in NC soil is deeper than that in uniform soil.

ACKNOWLEDGEMENTS

The work described here is supported by Discovery Grant from Australian Research Council (Grant No. DP0344019) and Natural Science Foundation of China (Grant No. 50309001). These supports are gratefully acknowledged.

REFERENCES

Boroomand, B. and Zienkiewicz, O. C. (1997). *An improved REP recovery and the effectivity robustness test*. International Journal for Numerical Methods in Engineering. 40, 3247-3277

Das, B. M. (1980). *A procedure for estimation of ultimate capacity of foundations in clay*. Soils and Foundations. 20(1), 77-82

Das, B. M. and Singh, G. (1994). *Uplift capacity of plate anchor in clay*. Proc. 4th ISOPE, Osaka, Japan. 436-442

Hu, Y. and Randolph, M. F. (2002). *Bearing capacity of caisson foundations on normally consolidation clay*. Soils and Foundations. 42(5), 71-77

Martin, C. M. and Randolph, M. F. (2001). *Application of the lower and upper bound theorems of plasticity to collapse of circular foundations*. Proc. 10th ICCMAG, Tucson, USA. 1417-1428

Merifield, R. S., Lyamin, A. V., Sloan, S. W. and Yu, H. S. (2003). *Three-dimensional lower bound solutions for stability of plate anchor in clay*. Journal of Geotechnical and Geoenvironmental Engineering. 129(3), 243-253

Merifield, R. S., Sloan, S. W. and Yu, H. S. (2001). *Stability of plate anchors in undrained clay*. Geotechnique. 51(2), 141-153

Rowe, R. K. and Davis, E. H. (1982). *The behaviour of anchor plates in clay*. Geotechnique. 32(1), 9-23

Song, Z. and Hu, Y. (2005). *Vertical pullout behavior of plate anchors in uniform clay*. Proc. ISFOG, Perth, Australia. 205-211

Song, Z., Hu, Y., Wang, D. and O'Loughlin, C. (2006). *Pullout capacity and rotational behaviour of square anchors*. Proc. 6th ICPMG, Hongkong, China. 1325-1331

Wilde, B., Treu, H., Fulton, T. (2001). *Field testing of suction embedded plate anchors*. Proc. 11th Int. Offshore and Polar Engineering Conf., Stavanger, Norway, 544-551.